

# Effects of Initial Condition and Cloud Density on the Composition of the Grain Mantle

Ankan Das<sup>1,2</sup>, Kinsuk Acharyya<sup>2</sup>, Sandip K. Chakrabarti<sup>2</sup>

<sup>1</sup>*Indian Centre for Space Physics, Chalantika 43, Garia Station Rd., Kolkata, 700084, India*

<sup>2</sup>*S. N. Bose National Centre for Basic Sciences, Salt Lake, Kolkata 700098, India*

## ABSTRACT

Evolution of grain mantles in various interstellar environment is studied. We concentrate mainly on water, methanol, carbon di-oxide, which constitute nearly 90% of the grain mantle. We investigate how the production rates of these molecules depend on the relative gas phase abundances of oxygen and carbon monoxide and constrain the relevant parameter space which reproduces these molecules closed to the observed abundances. Allowing to accrete only H, O and CO on the grains and using the Monte-Carlo method we follow the chemical processes for a few million years. We allow formation of multi-layers on the grains and incorporate the freeze-out effects of accreting O and CO. We find that the formation of these molecules depends on the initial conditions as well as the average cloud density. Specifically, when the number density of accreting O is less than 3 times more than that of CO, methanol is always over-produced. Using available reaction pathways it appears to be difficult to match the exact observed abundances of all the three molecules simultaneously. Only in a narrow region of parameter space all these three molecules are produced within the observed limit. In addition to this, we found that the incorporation of the freeze-outs of O and CO leads to almost steady state on the grain surface. The mantle thickness grows anywhere between 60 to 500 layers in a period of two million years. In addition, we consider a case where the gas number density changes with time due to gradual collapse of the molecular cloud and present the evolution of composition of different species as a function of radius of the collapsing cloud.

**Key words:** Molecular clouds, ISM, abundances, molecules, chemical evolution, Monte-Carlo simulations

## 1 INTRODUCTION

The study of chemical evolution of interstellar medium is well recognized to be a challenging task. Interstellar medium (ISM) is a rich reservoir of complex molecules. So far, around 150 gas phase molecules and around 20 molecular species on the grain surface have been detected in the various regions of ISM, especially in the regions of star formation. In the last decade, it was well established that the gas phase reactions alone cannot explain the molecular abundances in the ISM. The chemical reactions which occur on the interstellar dust grains are essential to explain the formation of several molecules especially hydrogenated species including the simplest and the most abundant molecule  $\text{H}_2$ . Interstellar grains provide the surface for the accreted species to meet and react. Therefore, an understanding of the formation of molecules on the grain surfaces is of prime importance. In this paper, we mainly follow the evolution of the grain mantle as a function of the initial condition. We concentrate only on water, methanol and carbon di-oxide, since they constitute nearly 90% of the grain material in dense regions of ISM. These molecules are detected on the grain surface due to their strong absorption bands arising out of multiple vibrational modes. Water is the most abundant species on a grain in the dense interstellar medium. It has an abundance of  $10^{-4}$  with respect to the total hydrogen column density (Tielens et al. 1991). The ice band, at  $3.07 \mu\text{m}$  ( $3280 \text{ cm}^{-1}$ ) is due to the O-H stretch mode of  $\text{H}_2\text{O}$  ice and it was first discovered by Gillett & Forrest (1973) in BN objects.  $\text{CO}_2$  is the second most abundant molecule in the interstellar medium with an abundance of around 20% with respect to  $\text{H}_2\text{O}$ . However, this abundance can vary from cloud to cloud and in clouds like W 33A it could be even less than 5% of water abundance (Keane et al. 2001). Several strong  $\text{CO}_2$  features are observed (de Graauw et al. 1996; Keane et al. 2001). Generally, it is found that the  $\text{CO}_2$  correlates best with  $\text{H}_2\text{O}$  ice, revealing the fact that these molecules may have similar chemical history. The next most abundant molecule is  $\text{CO}$ , which is the well studied ice with an abundance varying between 2% to 15% of water and with a characteristic absorption feature near  $2140 \text{ cm}^{-1}$  ( $4.67 \mu\text{m}$ ). The next strong feature is due to methanol ( $\text{CH}_3\text{OH}$ ), its abundance could vary between 2% to 30% of water. However, in most of the cloud it is less than 10%. Observed abundances around a few clouds are used from Keane et al. (2001) and references therein.

Hollenbach & Salpeter (1970), first introduced the grain surface chemistry to explain the formation of molecular hydrogen. Since then it has been used very widely by several authors (Watson & Salpeter 1972a,b; Allen & Robinson 1975, 1976, 1977; Tielens & Hagen

1982; Hasegawa et al. 1992; Charnley 2001; Stantcheva et al. 2002; Acharyya et al. 2005; Biham et al. 2001; Chakrabarti et al. 2006a; Green et al. 2001; Das et al. 2008a,b). These studies mainly belong to two different categories, namely, the deterministic approach and the stochastic approach. In the deterministic approach, one can completely determine the time evolution of the system once the initial conditions are known. Rate equation method belongs to this category. This method is very extensively used by several authors to study the grain surface chemistry (Herbst & Klemperer 1973; Prasad & Huntress 1980; Hasegawa et al. 1992; Roberts & Herbst 2002). However, this method is only applicable when there are large number of reactants on the grain surface. Given the fact that the interstellar medium is very dilute, very often this criteria is not fulfilled and this method cannot be applicable. But this method is computationally faster and can very easily be coupled with the gas phase reactions. In the stochastic approach, fluctuations in the surface abundance due to the statistical nature of the grain is preserved. The Monte Carlo method and the Master equation methods belong to this category. Both these methods are used by several authors (Charnley 2001; Green et al. 2001; Biham et al. 2001; Stantcheva et al. 2002). Its major disadvantage is that it is computationally intensive. Coupling of Monte-Carlo method to study grain surface reactions and rate equation method for gas phase reactions is extremely difficult. The Master equation method can be coupled with the rate equations, however, it is disadvantageous because for a large network one had to solve a large number of reactions

Recently, Chang et al. (2005) argued that the stochastic methods used so far can also lead to error because the rate of reaction is determined by the rate of hopping (or tunneling) of a hydrogen atom from one site to the nearest neighboring site multiplied by the probability of finding a reactant partner in this site. This is also an average treatment since on any given grain the reactant partner is unlikely to lie in the nearest-neighboring site. They used a continuous random walk technique to study the formation of molecular hydrogen. Chakrabarti et al. (2006a,b) used a similar method which keeps track of each individual reactant and their movements and calculated effective grain surface area involved in the formation of molecular hydrogen in the interstellar clouds. Furthermore, they defined an important parameter called ‘catalytic capacity’ which measures the efficiency of the formation of  $H_2$  on a grain surface for a given pair of H residing on it. They studied the formation of water and methanol up to a mono-layer and estimated the abundances of these two molecules. They found that the formation rate of various molecules is strongly dependent

on the binding energies, number density in the gas phase, effective grain surface area and on the formation mechanism Das et al. (2008b).

In this we paper, we first vary the elemental abundances of O and CO and found regions in which these molecules are produced efficiently. We then changed the cloud density and found how the abundance is affected. In Section 2, we discuss various physical processes that are involved during a gas-grain interaction. In Section 3, we describe the methodology of our calculations. In Section 4, we describe our model and the nature of the initial conditions. In Section 5, the results are presented. Finally, in Section 6, we draw our conclusions.

## 2 MECHANISMS OF REACTIONS ON GRAIN SURFACES

There are four physical processes that are involved while gas phase atoms/molecules interact with the grains. The first step is ‘accretion’, i.e., landing of various species onto a grain. In our case only H, O and CO are considered as accreting species onto the grain surface. The second step is ‘hopping’ through which the accreted species move around the grain. In the third step, the accreted species will react to form various new species either through the Langmuir-Hinselwood (LH) mechanism or by the Eley-Rideal (ER) mechanism. In the LH scheme, the gas phase species accreted onto a grain becomes equilibrated with the surface before it reacts with another atom/molecule, and in the ER reaction scheme, incident gas phase species collides directly with an adsorbed species on the surface and reacts with that species. In such a mechanism, generally the reactant does not become trapped at the surface and it is unlikely to be sensitive to the surface temperature (Farebrother et al. 2000). In our study, we take it that the reactions on a surface can occur through both LH and ER mechanisms. However, we assume that the molecules remain trapped after reactions due to their high binding energy. Typical temperature of dense cloud is around 10 K, and in this temperature only hydrogen can desorb at a meaningful rate. All the other molecules stay on the grain until these grains are heated up. When the temperature of the grain is increased, these molecules desorb back into the gas phase according to their binding energy of desorption.

We define the accretion rate  $[r_{acc}(i)]$  of a given neutral species  $i$ , in the units of  $\text{s}^{-1}$ , as,

$$r_{acc}(i) = S_i \sigma v_i n_i, \quad (1)$$

where,  $S_i$  is the sticking coefficient (taken as 1 for all the three species),  $v_i$  is the velocity ( $\text{cm s}^{-1}$ ),  $n_i$  is the number density of the  $i$ -th species in the gas phase and  $\sigma$  is the grain cross-

section ( $\text{cm}^2$ ). Since we have carried out our calculations for three different cloud densities and different initial abundances we have used many sets of accretion rates. Number densities for different clouds are taken from Stantcheva et al. (2002) and are listed in Table 1. Number density of hydrogen in gas phase is denoted by  $n_h$  and the number density of O and CO with respect to hydrogen number density is expressed as  $n_O$  and  $n_{CO}$  respectively.

The binding energy of the incoming species greatly depends on the species itself and on the way the interactions proceeded. The incoming species might get trapped inside a shallow potential well at a physisorbed site. The interaction is mainly due to mutually induced dipole moments. A strong covalent bond may also be formed through chemisorption. Recent studies have found the evidences of both physisorption and chemisorption processes Cazaux and Tielens (2002). However, for the chemisorption, high kinetic energy is involved and hence this type of interaction is not relevant except in a very special astrophysical conditions. Therefore, we considered only weakly bound species, i.e., physisorbed atoms and molecules. The typical energy for physisorption is around 0.1 eV or  $\sim 1000$  K. Let us denote the binding energy for physical adsorption by  $E_D$  and,  $E_b$ , the potential energy barrier which must be tackled in order that the species diffuses from one site to other. We need many interaction energies to describe the system completely, not just among the silicate surfaces and adsorbed species but also among the adsorbed species themselves. Table 2, contains all the binding energies that are used in our calculation. However, binding energies are not known with certainty. We took the binding energies of H and  $\text{H}_2$  on the silicate surface from Katz et al. (1999), the binding energies of other species with bare silicate grain from Allen & Robinson (1977); Tielens & Allamandola (1987); Hasegawa et al. (1992), and the binding energies among H, O, OH and  $\text{H}_2\text{O}$  from Cuppen & Herbst (2007). For the rest, we kept the energies same as those on the silicate surface. These are taken from Hasegawa & Herbst (1993).

For a chemical reaction to occur, an accreted species has to scan the surface in search of a reaction partner. There are two physical processes which can provide the mobility for the accreted gas phase species, namely, the thermal hopping and tunneling. As mentioned earlier, Hollenbach & Salpeter (1970) first introduced the grain surface chemistry to explain the high abundance of molecular hydrogen. They assumed that within the grains, hydrogen atoms move from site to site by quantum mechanical tunneling process. But from the recent experimental results of molecular hydrogen formation it was found that the mobility of hydrogen on grains is primarily due to thermal hopping (Pirronello et al. 1997a,b, 1999).

In the paper, we have considered the thermal desorption only. However, other than the hydrogen and hydrogen molecule no species desorbs at 10 K. Other molecules can come out of the grain surface only when the grains are heated up. Many different types of desorption mechanisms are present in the literature. In the dense cloud, the most important is impulsive heating of the grains (Hasegawa & Herbst (1993)) by the cosmic rays. However, this mechanism is effective for small molecules. Following Hasegawa & Herbst (1993), and assuming the binding energies of the species with water, we obtain the time scales for CO, O<sub>2</sub>, H<sub>2</sub>O, CH<sub>3</sub>OH and CO<sub>2</sub> are 10<sup>14</sup> sec, 10<sup>14</sup> sec, 3 × 10<sup>41</sup> sec, 2 × 10<sup>19</sup> sec and 10<sup>22</sup> sec respectively. Thus the cosmic ray induced desorption mechanism is completely in-effective for H<sub>2</sub>O, CH<sub>3</sub>OH and CO<sub>2</sub> and weakly effective for CO and O<sub>2</sub> at much later time. In addition to this, Shen et al. (2004) argued that Hasegawa & Herbst (1993) over-estimated the rate as they assumed that the sublimation of the volatile species such as CO occurs near 70K, but it is not possible for the Cosmic ray particle to heat a bigger grain (due to dust accretion the size of the grain in fact increases) upto such high temperature. Finally Shen et al. (2004) concluded that the CR induced UV field is about 10 times more efficient in depositing energy in the ice than the direct CR energy deposition. So if we scale our calculated time scale of desorption accordingly, we can conclude that it is again in-effective for H<sub>2</sub>O (~ 3 × 10<sup>40</sup>sec), CH<sub>3</sub>OH (~ 2 × 10<sup>18</sup>sec) and CO<sub>2</sub>(10<sup>21</sup>sec). For CO and O<sub>2</sub> it is ~ 10<sup>13</sup>sec ~ 10<sup>6</sup>year, which is our simulation time scale. So we can conclude that inclusion of these desorption mechanism will not significantly affect our results. Garrod et al. (2007), suggested a new type of desorption mechanism in which they used exothermicity of surface addition reaction to desorb product molecules from the surface. They used this mechanism parametrically for gas-grain interaction code and found that the maximum desorption due to this mechanism is 10 %. It is important only at later times (after 3-4 Million years). Therefore, we have not included this type of desorption in our computation.

Along with the physical processes one also needs to know what are the reaction pathways which can lead to the formation of these molecules. All the reaction pathways that are considered in our study are listed in Table 3. We assume that water is formed through  $H + O \rightarrow OH$ ,  $H + OH \rightarrow H_2O$  (Eq. 2 and 3) (Hasegawa et al. 1992; Stantcheva et al. 2002). Recently, Ioppolo et al. (2008), suggested formation of water through  $H + O_2$  channel in which O<sub>2</sub> is converted to H<sub>2</sub>O via H<sub>2</sub>O<sub>2</sub>. However, considering that water is the most abundant species on a grain surface and there is very little observed O<sub>2</sub> and H<sub>2</sub>O<sub>2</sub>, we have not considered this path way. Methanol formation through hydrogenation is studied by

three groups (Hiraoka et al. 2002; Watanbe & Kouchi 2002; Fuchs et al 2009). Hiraoka et al. (2002) observed only formaldehyde formation, whereas Watanbe & Kouchi (2002) also found efficient methanol production. These two groups presented these apparently contradicting results in a series of papers and this discrepancy was mainly attributed to be a result of different experimental conditions, especially on H-atom flux. Fuchs et al (2009), found that the formation mechanism of formaldehyde and methanol does not fundamentally change with varying flux and concluded that the surface hydrogenation of CO can safely be used to explain the majority of the formed methanol in the interstellar medium. We have also considered methanol formation through successive hydrogenation of CO through Eq. 4, 5, 6 and 7. Among these, Eqs. 4 and 6 have an activation barrier of 2000 K. O<sub>2</sub> is formed through Eq. 9. Finally, CO<sub>2</sub> is formed through Eq. 9 and 10 Stantcheva et al. (2002).

### 3 PROCEDURE

We have used continuous-time random walk Monte Carlo method to study the evolution of grain mantle. For the sake of simplicity, we take all the grains to be of square shaped and assume that each site has four nearest neighbors, as in an fcc[100] plane. In order to mimic the spherical grain structure, we assume periodic boundary condition i.e., a species which leaves the simulation grid from one boundary enters back from the opposite boundary. In the earlier Section, we discussed all the steps which occur on a grain surface and we implemented these steps in following way: In the first step, we drop atoms/molecules after every  $1/r_{acc}$  seconds. Since we are considering three different species we have three different accretion rates for each species depending on the number densities. Typically, for a cloud of intermediate number density and a classical grain it is  $1.2 \times 10^5$  seconds (order of a day),  $7.5 \times 10^6$  seconds ( $\sim$  couple of months) and  $8.75 \times 10^5$  seconds ( $\sim$  weeks) for H, O and CO respectively at the beginning. The location of the accreting  $i$ -th species is dictated by a pair of random numbers  $(R_x, R_y)$  obtained by a random number generator. This pair would place the incoming species at  $(j, k)^{th}$  site of the grain, where  $j$  and  $k$  are the nearest integers obtained using Int function:  $j = int(nR_x + 0.5)$  and  $k = int(nR_y + 0.5)$ . Here,  $n = \sqrt{s}$ , where,  $s$  is the number of sites on the grain. We have considered  $50 \times 50$  grain. It was found by Chang et al. (2005) that when the size of the simulated surface is at least  $50 \times 50$  there is no size effect. We then scaled the result for classical grains ( $\sim 10^6$  sites). While considering the grain mantle formation in multilayer regime, two possibilities may occur depending on

whether the site is already occupied or not. If the site is not occupied, then the accreted species can sit on the surface of the bare silicate grain at the randomly generated  $(j, k)^{th}$  location. But if the site is occupied then either a reaction between the incoming and the stationary species will occur, provided the reaction is permitted (ER mechanism) and will form a new molecule or it can diffuse through the grain according to the binding energy with species. In the second step, all the accreted species are allowed to hop. We choose  $1/a_h$ , the hopping time of hydrogen as the minimum time step and advance the global time by this time step. Hopping time of H, O and CO with the silicate surface at 10 K is  $7.5 \times 10^{-7}$  second, 0.02 seconds and 6000 seconds respectively. Since, CO hopping time is much higher with respect to O and H, we have not considered the hopping of CO.

It is generally observed that the hopping time scale is many order of magnitude smaller than the accretion time scale. Therefore, once one H or O lands on a grain surface, it can scan the grain very efficiently and react almost instantaneously due to the thermal hopping. Tunneling also provides a mobility to hydrogen atoms but it is much faster than hopping. Therefore, inclusion of tunneling means that the scanning can proceed even faster. But as the accretion time scale is not altered, we will not have any major differences in our result. Already in Das et al. (2008b), we did not find any major difference between the results obtained with the hydrogen tunneling and the hydrogen hopping. (Pirronello et al. 1997a,b, 1999) did not find the experimental evidence of tunneling either. However, many models, e.g., Cazaux et al. (2008), still use tunneling for the mobility of hydrogen atoms.

In an fcc[100] plane there are four directions to hop. We generate random numbers for the four nearest neighbor of the diffusing species to decide the direction  $(n, l)$  of it. Here we are considering all the situations by the Markov chain Monte Carlo method which is a random walk process and the walker will often move back and cover the place already covered. So by considering this we automatically include the back-diffusion probability mentioned by Chang et al. (2005). Once again, two possibilities may occur: If the site is occupied then either it will react when the reaction is permitted or it will wait until the next hopping time. If the neighboring site is vacant and it does not have any species just beneath that site then it can roll down on that  $(n,l)^{th}$  grid until it touch some species or the bare grain surface. If the reaction between the species and the diffusing species is permitted, a new species is formed and if not, then it can sit on the top of that. From Table 2, it is to be noted that some species are very weakly bound with the other surface species such as, O with  $O_2$ . Since, the hopping probability is higher than that of the evaporation, it is most likely that the species

will drop down from the top of the weak binding species rather than evaporating from there. Finally, the species are desorbed back into the gas phase. This is also done by generating random numbers. Actually, after each hopping we generated a random number to decide if the species will hop or desorb. We have evolved our system up to a few million years, which is typical life time of a molecular cloud.

In Das et al. (2008b), the simulations were restricted in the mono-layer regime. Therefore, it was not possible to study the evolution and composition of the grain mantle with time. In this paper, we used binding energies not just between the different species with the bare olivine substrate but also with ice and with the other adsorbed species. In fact, we considered all possible binding energies to describe the system. In addition to this, we also considered the freeze out of O and CO from the gas phase. These are the major improvement with respect to our previous model. Cuppen & Herbst (2007) and Cuppen et al. (2009), also considered the formation of grain mantles. However, Cuppen & Herbst (2007), restricted themselves only to the formation of water and Cuppen et al. (2009) restricted themselves only to the formation of methanol. They did not study the variation as function of initial abundances. We have extended the study of grain mantle by incorporating all the major grain surface species namely, H<sub>2</sub>O, CH<sub>3</sub>OH and CO<sub>2</sub> and CO which contains nearly 90 % of grain mantle composition and we have studied the variation of the abundances with respect to the initial conditions and cloud densities.

#### 4 MODEL

In our calculation, only three gas phase species, namely, H, O and CO are allowed to accrete on a silicate grain surface. In total, on a grain surface, 10 chemical reactions are considered which can occur among these three constituents via thermal hopping. H<sub>2</sub>, O<sub>2</sub>, H<sub>2</sub>O, H<sub>2</sub>CO, CH<sub>3</sub>OH, and CO<sub>2</sub>, as well as reactive intermediate species are formed. No gas phase chemistry is considered and the initial gas-phase concentrations of only CO and O are varied from Model to Model while the hydrogen concentration is assumed to be constant. This will decrease the accretion rate of O and CO species with time. In other words, freeze out effect of these two molecules are taken into account. Because of this effect, the accretion rates of these molecules decrease and the number of these species on the grain surface will also decrease. This will, in turn, result in a decrease in the formation rate of molecules which uses them.

We consider conditions which are representatives of a dense cloud. In these clouds, most of the atomic hydrogen is converted into molecular hydrogen and atomic carbon into CO via gas phase chemistry. Therefore, we have considered accretion of CO instead of atomic carbon. The abundances ( $\text{cm}^{-3}$ ) of H, O, and CO are shown in Table 1. These values were obtained from steady-state gas-phase model runs at total hydrogen number densities ( $n_h$ ) of  $10^3$ ,  $10^4$ , and  $10^5 \text{ cm}^{-3}$  taken from Stantcheva et al. (2002). We designate them as ‘low’, ‘intermediate’ and ‘high’ density cases. Furthermore, we have varied the initial abundances of O ( $n_O$ ) and CO ( $n_{CO}$ ) for intermediate density case to see the effects. We have shown earlier that the methanol and water can be efficiently formed in the clouds of intermediate density (Das et al. (2008b)). We scan the entire parameter space to find favourable conditions for the production of water, methanol and carbon di-oxide. We varied the O abundance between  $7 \times 10^{-5}$  and  $7 \times 10^{-4}$  and CO between  $7.5 \times 10^{-6}$  and  $1.5 \times 10^{-4}$  with respect to the total hydrogen. SWAS findings of very low  $\text{H}_2\text{O}$  and  $\text{O}_2$  put a serious concern over the gas phase O abundance. Gas and solid state molecules can account about 55 % of the oxygen (Bergin et al. (2000)). Therefore, remaining atomic oxygen is in the gas phase as was found toward a few sources ((Caux et al. 1999; Lis et al. 2001) and references therein). Another possibility is that there is a higher depletion of atomic oxygen onto the dust grain. Bergin et al. (2000), found that using a  $\text{C}/\text{O} > 0.9$ , they can re-produce the SWAS observations of  $\text{H}_2\text{O}$  and  $\text{O}_2$  abundance in star forming cores. We have chosen lower limit of O abundance such that we have  $\text{C}/\text{O}$  ratio close to 1. Atomic oxygen abundance as high as  $7 \times 10^{-4}$  is used to mimic the conditions around solar neighborhood. We have chosen the CO initial abundance on the basis of various available studies (Jørgensen et al. 2002; Wilson and Rood 1994). We have considered the grain temperature to be at 10 K. In this temperature, only H, O and  $\text{H}_2$  have mobility and CO is almost immobile, therefore we have neglected the hopping of CO thereby saving the computational time. We presented in this paper a few selected results out of our many model runs.

## 5 RESULTS

We found that the formation of water, methanol and carbon dioxide on a grain surface strongly depends on initial gas phase abundances of O and CO and on the cloud density. Initial abundance and cloud density dictate the relative accretion rates of O and CO thereby controlling the formation of these molecules.

### 5.1 Variation of abundance due to initial abundance

In Fig. 1(a-l), we show the variation of abundances of selected species as a function of time for different initial conditions and for intermediate cloud density, i.e., the total hydrogen number density is  $10^4 \text{ cm}^{-3}$ . We vary the gas phase atomic abundance between  $7 \times 10^{-5}$  and  $7 \times 10^{-4}$  and CO abundance between  $7 \times 10^{-5}$  and  $1.5 \times 10^{-5}$  with respect to the total hydrogen number density. Table 4, summarizes abundances of these molecules after two million years. In Fig. 1a, the initial O abundance of  $7 \times 10^{-5}$  and CO abundance of  $7.5 \times 10^{-5}$  were used. We find that under this condition there is more methanol than water. The reason is that the accretion rate of CO is little higher ( 7%) than O and it is mainly utilized to form methanol and  $\text{CO}_2$  whereas, O is utilized to form water,  $\text{O}_2$  and  $\text{CO}_2$ . The next most abundant molecule is  $\text{CO}_2$ . It is mainly formed through reaction number 10 in Table 3. We find that at around  $2 \times 10^6$  years, the rate of formation of these molecules slowed down significantly, this is because we have considered the freeze out effects of CO and O. As the number densities of these two species go down in gas phase, their accretion rates also go down which results in a decrease in the rate of formation of other molecules. When O and CO are heavily depleted from the gas phase, we obtain a near steady state on the grain surface. In Figs. 1b and 1c, we have decreased the initial CO abundance by a factor of half and one-fifth respectively for a fixed O abundance, which results in a decrease in methanol and an increase in water abundance. Water is accounted for nearly 60% and 80% of the grain mantle respectively. The methanol abundance is 52% and 20% with respect to water and  $\text{CO}_2$  is 9% and 3% respectively (Table 4).

At this stage, it is pertinent to ask that how close these results are to the observed values. We find that in almost all the cases methanol is over estimated and  $\text{CO}_2$  is under estimated (Keane et al. 2001). In Fig. 1d, we increase the abundance of O. The net affect is a decrease of methanol and a small increase in the abundance of molecular oxygen. Once again, if we compare this set with the observed value (Keane et al. 2001) we find that the abundance of water and  $\text{CO}_2$  is close to observed values. However, the methanol is over-produced. In Fig. 1e, we decreased the abundance CO by half, which results in a farther reduction of methanol. For this case, the abundance of methanol and water is in close agreement with the observed value in GL 7009S. However, abundance of  $\text{CO}_2$  is nearly half of the observed abundance. In Fig. 1f, CO abundance is one-fifth and  $\sim 90\%$  of the grain mantle is made up of water. It is understandable because with this initial condition, the accretion rate of O is

nearly one order of magnitude greater than CO. Next we increase the initial O abundance by five times (Fig. 1g). Once again, the water is the most abundant species, methanol and CO<sub>2</sub> is within the observed limit but a substantial increase in the abundance of molecular oxygen is seen. Thus a high abundance of molecular oxygen could be found in a oxygen rich environment. In Figs. 1h and 1f, results are shown for half and one-fifth CO abundance. The abundance of CO in most of the cases is very low. This is due to the fact that CO in a grain is rapidly converted into methanol and CO<sub>2</sub>. Finally, we have increased the O abundance 10 times and found a substantial increases in molecular oxygen abundance (Fig. 1j, 1k and 1l).

In Fig. 2, a cross-sectional view of the mantle structure after one million year is shown. The O abundance of  $1.05 \times 10^{-4}$  and CO abundance of  $1.5 \times 10^{-5}$  were used in the simulation. In this case, water forms about 85% of the grain mantle, methanol about 13% and CO<sub>2</sub> about 3% of water. Total number of mono-layer formed is 85. The species having less than 1% surface coverage are not shown in the Figure.

In Fig. 3 and Fig. 4, we show the variation of final mantle abundance of selected species as a function of initial abundance of gas phase O and CO. This Figure is analogous to Fig. 1. In Fig. 1 we have shown as a function of time and in these two figures we have plotted abundances of selected species as a function of accreted gas phase O abundance and CO. In Fig. 3, each column represents a fixed value of CO:  $7.5 \times 10^{-5}$  (1st column),  $3.75 \times 10^{-5}$  (2nd column) and  $1.5 \times 10^{-5}$  (3rd column) with respect to total hydrogen number density and initial gas phase O abundances ranging from  $7 \times 10^{-5}$  to  $7 \times 10^{-4}$  with respect to total hydrogen number density. Purpose of this plot is to get an idea of how absolute abundance changes with initial condition. With increasing gas phase O, production of oxygenated species like H<sub>2</sub>O, O<sub>2</sub> and CO<sub>2</sub> increases whereas the production of methanol decreases. Grain phase CO also less populated with the increase in initial gas phase O as CO are mostly converted to CO<sub>2</sub>. In Fig. 4, we choose initial gas phase O to be  $7 \times 10^{-4}$  (1st column),  $1.05 \times 10^{-4}$  (2nd column) and  $7 \times 10^{-5}$  (3rd column) and show the final abundances of various species at the grain mantle for different initial gas phase CO abundances ranging from  $1.5 \times 10^{-5}$  to  $3.5 \times 10^{-4}$ . It is clear from the Figure that as the initial gas phase CO abundance increases, methanol production increases. Due to the enhance hydrogenation of CO for the production of methanol, production of H<sub>2</sub>O decreases which result some O free enough to react with other O or CO to produce O<sub>2</sub> or CO<sub>2</sub>. So O<sub>2</sub> and CO<sub>2</sub> also increases with the increase in the gas phase CO abundances.

### 5.1.1 Grain mantle thickness

In Fig. 5, we show the time evolution of the number of mono-layers. Time evolution of the number of layer is shown for initial gas phase  $\text{CO}=7.5 \times 10^{-5}$ ,  $3.75 \times 10^{-5}$  and  $1.5 \times 10^{-5}$  and for different gas phase O noted on the right side of the box. It is found that the mantle thickness is a function of initial gas phase abundance and thickness varies between 60 to 500 mono-layers. For higher initial abundance, accretion rate is high, which results higher mantle thickness on the grain because now grain has more matter to process.

### 5.1.2 Parameter space and zone of interest

By varying the initial abundances of O and CO we find that in almost all the cases, water is the most abundant species. The next most abundant species is the methanol which is generally contrary to the various observational results. Next most abundant species is  $\text{CO}_2$  which is generally close to the observed values. This prompted us to run our code for a wide set of parameters to find out parameter space in which these molecules are produced in the observed range. Results are presented in Figs. 6a, 6b and 6c. We plot water, methanol and  $\text{CO}_2$  coverages on the grain mantle as a function of initial abundances of O and CO and marked the zone in which these molecules are within the observed limit. We call this as a favourable zone. Thus the favourable zone excludes abundances which are over produced or less produced with respect to the observed limit. Observed limits are selected using Keane et al. (2001). To find out the favourable zone we considered those cases for which at least 80 mono-layers are formed, water abundance is around  $10^{-4}$ , methanol abundance is between 2% – 30% of the solid state water and  $\text{CO}_2$  abundance between 2% and 20% of the solid state water. We find that the water abundance is close to observed value when CO abundance is less than  $5 \times 10^{-5}$  and O is between  $3.5 \times 10^{-5}$  and  $7 \times 10^{-4}$ . Methanol is close to observed value when CO abundance is between  $7.5 \times 10^{-6}$  and  $1.5 \times 10^{-4}$  and O is between  $3.5 \times 10^{-5}$  and  $7 \times 10^{-4}$ . Similarly, with  $\text{CO}_2$ , this zone for CO is between  $1.5 \times 10^{-5}$  and  $7.5 \times 10^{-5}$  and O between  $3.5 \times 10^{-5}$  and  $7 \times 10^{-4}$ . In Fig. 6d, we have superimposed favourable zones from all the three species to see whether there is any region which is common to all the three favourable zones. It is clearly seen that only in a very narrow region of the parameter space, the observed abundance could be roughly reproduced.

### 5.1.3 *Effect of the activation energy*

We have performed another exercise by increasing the activation energy of methanol formation to check if this could reduce methanol formation. We increase the activation barrier energy by a factor of 1.5, 2 and 2.5 times with respect to the activation energy barrier used by several authors. An increase in activation energy up to two times has almost no effect on methanol production. However, when the activation energy is 5000 K (2.5 times higher) we find a dramatic reduction of methanol formation (Table 5). This also reduces CO<sub>2</sub> production because the efficient formation route for CO<sub>2</sub> in our method is found to be the reaction no. 10 of Table 3. Under this condition, a lot of unused CO remains on the grain and an enhanced production of CO is observed.

## 5.2 **Variation of abundance with cloud density**

In Fig. 7, we plot the abundance of selected species as functions of time for various cloud density for initial abundance shown in Table 1 and result is tabulated in Table 6. In the low density case only water and methanol is produced efficiently and the abundance is also not close to the observed value. In the intermediate case, the most abundant species is methanol rather than water. A reasonably good amount of CO<sub>2</sub> is also produced. Finally, in the high case, everything is heavily produced, especially those requiring CO in the reaction scheme. This is because under this condition hydrogen supply to saturate CO is insufficient. Our general conclusion is that by varying cloud density and using standard formation route of water and methanol it is difficult to reproduce the observed abundances for these molecules.

## 5.3 **Collapsing cloud**

In a realistic molecular cloud, the density will change with time due to a gradual collapse of the cloud. To understand how the abundance of various species changes with density we now consider a cloud which collapses with time. However, since coupling of the grain chemistry and a gas chemistry in presence of a collapsing cloud is a very difficult task we made some simplification. For simplicity, we use the radial density distribution from Das et al. (2008a), where a spherically symmetric, self gravitating, isothermal, collapsing cloud was considered. Initially this cloud is assumed to have a negligible amount of mass. The outer boundary is at 1 parsec and the inner boundary is at  $10^{-4}$  parsec. The matter which crosses the inner boundary is assumed to form the core. Matter is injected at a constant rate at the outer

boundary. In Das et al. (2008a), the cloud was divided into 100 logarithmically equal spaced grids. Here, we consider only 5 shells, each containing 20 grids. We take volume average of number densities in each shell to have an average density. We have taken the initial number density of various species to be same as it was for  $10^3\text{cm}^{-3}$  (low density, Table 1). Time evolution of the number density for a collapsing cloud is shown in Fig. 8a. The system is evolved with time due to collapse and incorporating the freeze-out and desorption effects. Abundance of a few selected species are shown in Fig. 8b where the five data points from the five shells could be seen. Methanol is varying between 60 % and 100 % of water, a signature we observed when cloud density was varied. Thus methanol is always over-produced. Deep inside the cloud, the methanol abundance begins to drop due to the unavailability of H atoms.  $\text{CO}_2$  is produced within the observed limit between outer shell to middle shells. However, as we go deep inside the cloud  $\text{CO}_2$  is heavily produced. Very little  $\text{O}_2$  is produced up to middle shells but a very good amount of  $\text{O}_2$  is produced deep inside the cloud. We found that as the density increases, H atom is rapidly used up due to hydrogenation reaction. As a result, we found  $\text{H}_2\text{O}$  and  $\text{CH}_3\text{OH}$  is produced very efficiently in the outer shells. In the process, as the cloud collapses, the relative numbers of CO and O go up with respect to H atom. This then favours the formation of  $\text{CO}_2$  and  $\text{O}_2$  in the inner shells. This resembles the abundances we obtained by varying cloud density. Thus once again we can conclude that the final abundances of the interstellar species are strongly dependent on the relative initial abundances of its constituents.

#### 5.4 Comparison with previous works

In Das et al. (2008b), water and methanol formations in a mono-layer on grain surfaces were studied, where freeze-out effects of gas phase species were not considered. In the present paper, we study the evolution of the mantle up to several tens of layers in presence of freeze-out effects. We also identify the parameters space in which the produced water, methanol and carbon dioxide are comparable to what are observed.

We have compared our results with that obtained from the rate equation method of Hasegawa et al. (1992). This we present in Fig. 9. We put ‘(m)’ for Monte-carlo method and ‘(r)’ for rate equation method. We found that the difference between the Monte-Carlo method and the rate equation method is negligible for  $\text{H}_2\text{O}$  and  $\text{CH}_3\text{OH}$ . However, for the species with smaller abundances, the differences are significant. For instance, our production of  $\text{CO}_2$

on grains via Eq. 10 of Table 3 is more efficient (than that via Eq. 9) where HCO is a reactant. In the rate equation method, it is likely that CO<sub>2</sub> would be estimated incorrectly due to very low abundance of HCO on the grain. This is reflected in Fig. 9 also. Discrepancies in other species can be similarly explained. The species with higher abundances are not affected because the rate equation method is valid in this regime. In this regard we can compare our results with some other previous works. Stantcheva et al. (2004) considered a gas-grain coupled network to study the chemical evolution of a static molecular cloud. Similar to our approach, their model also seems to be efficient for the production of methanol. Major differences between our results are that at the end we are obtaining significant amount of solid CO and CO<sub>2</sub>, where their result shows virtually no solid CO and little solid CO<sub>2</sub>. In Ruffle & Herbst (2000), a complete network of surface reactions were considered to study the quiescent source in front of the field star Elias 16, they were able to reproduce the CO abundances and upper limit to the Methanol abundances by considering much lower diffusion rates than the diffusion rates used here. However, all of their model were unable to produce significant about of CO<sub>2</sub>.

While comparing our results with other multilayer methods, we note that, Cuppen & Herbst (2007), studied the formation of water on grain surface for diffuse, translucent and dense clouds. The most striking difference of Cuppen & Herbst (2007) with the present work is that they did not include methanol formation at all. In our case, the H atom is partially used up to form methanol. Furthermore, in the absence of a few important species on the grain, such as methanol, carbon monoxide etc. they always found that water dominates the grain mantle. On the contrary, we found that for  $C/O \geq 1$ , methanol is produced more than water. Recently, Cuppen et al. (2009), studied the surface formation of CH<sub>3</sub>OH and H<sub>2</sub>CO from precursor CO using the continuous-time, random walk Monte-Carlo method. They found the formation of both the species to be very efficient and the efficiency depends mainly on the grain temperature and the abundance ratio of H and CO in the gas phase. They also found that the freeze-out of CO favours more complete hydrogenation of CO to form CH<sub>3</sub>OH. We found, indeed the methanol is formed very efficiently. However, in most of the cases formaldehyde in our case is less than 1% while it is somewhat higher in Cuppen et al. (2009). Another difference with Cuppen et al. (2009) is that we have considered the accretion of O also on the grain surface and thus we find that some fraction of the mantle is covered with O<sub>2</sub> and CO<sub>2</sub>. Varying the initial cloud composition (by changing the initial gas phase O and CO), we have noticed that in a narrow region of parameter space (Fig. 6d) our

model is producing  $\text{H}_2\text{O}$ ,  $\text{CO}_2$ , and  $\text{CH}_3\text{OH}$  within the observed limit. In the other regions of the parameter space we are getting an anti-correlation between the production of  $\text{CH}_3\text{OH}$ ,  $\text{CO}_2$  with  $\text{H}_2\text{O}$ .

## 6 CONCLUSIONS

In this paper, we have carried out numerical simulations using continuous-time random walk Monte-Carlo method to investigate formation of water, methanol and  $\text{CO}_2$  as a function of the cloud density and the initial abundances of CO and O. We found that when the accretion rate of CO is more than O, methanol is the most abundant species on the grain surface. An increase in the accretion rate of O over CO, methanol abundance gradually goes down. When the accretion rate of O is 1.4 times that of the CO accretion rate, the water abundance is more than that of methanol, i.e, a cross over is seen. One has to increase O/CO by a factor of 3 to get a methanol abundance which is  $\sim 30\%$ , the maximum abundance of methanol seen in the molecular clouds (Keane et al. 2001). When we increase the accretion rate of O further, methanol starts to get reduced and this trend continues. When we increase the ration O/CO by a factor of more than 10, although water is the most abundant molecule on the grain surface, we observed a surge in  $\text{O}_2$  abundance. We scanned the entire parameter space and found that in the clouds having  $O/CO < 3$ , methanol is overproduced. This criteria is true only when there is no depletion, because we have more O than CO to start with. Once the accretion process sets in, the gas phase species will get depleted on to the grain and we will have clouds with different C/O ratio. The cloud conditions in which the C/O ratio is less than 0.33, water is found to be produced very efficiently on the grain surface. We concede that matching  $\text{CO}_2$  abundance with the observational results still remains a problem. We found that  $\text{CO}_2$  is mainly formed through reaction no. 10 in Table 3, i.e., it requires HCO to form. Therefore, conditions which lead to decrease in methanol formation also decrease the formation of  $\text{CO}_2$ . We have also checked the effects of increasing activation barrier energy for methanol formation, but the result is not improved as far as matching with observed abundances is concerned. We also failed to match with observed abundances by changing the cloud density only. However, when we super-impose the favourable formation zones of  $\text{H}_2\text{O}$ ,  $\text{CH}_3\text{OH}$  and  $\text{CO}_2$  we do obtain a narrow region in which all these molecules are produced within the observed limit. *To have more realistic estimation about the abundances of various interstellar species in the different regions of the molecular cloud, we have considered a*

*collapsing cloud and have coupled the time evolution of density distribution with our Monte Carlo approach of the grain chemistry. We have noticed that throughout the cloud  $CH_3OH$  is always overproduced. Deep inside the cloud  $CO_2$  and  $O_2$  are heavily produced whereas at the outer edge their production gradually decreases.*

## 7 ACKNOWLEDGMENTS

A. Das wishes to acknowledge the hospitality of S. N. Bose National Centre for Basic Sciences when the paper was written.

## REFERENCES

- Acharyya, K., Chakrabarti, S.K., Chakrabarti, S. 2005, MNRAS, 361, 550
- Allen, M., Robinson, G. W., 1975., ApJ, 195, 81
- Allen, M., Robinson, G. W., 1976., ApJ, 207, 745
- Allen, M., Robinson, G. W., 1977., ApJ, 212, 396
- Bachiller, R., Perez Gutierrez, M., 1997, ApJ, 487L, 93
- Bachiller, R., Codella, C., Colomer, F., Liechti, S., Walmsley, C. M., 1998, A&A, 335, 266
- Bergin, E. A. *et al.*, 2000, ApJ, 539, 129
- Biham, O., Furman, I., Pirronello, V., Vidali, G., 2001, ApJ, 553, 595
- Caux, E., *et al.* 1999, A&A, 347, L1
- Cazaux, S., Tielens, A. G. G. M., 2002, ApJ, 575, 29
- Chakrabarti, S.K., Das, A., Acharyya, K., Chakrabarti, S., 2006, A&A, 457, 167
- Chakrabarti, S.K., Das, A., Acharyya, K., Chakrabarti, S., 2006, BASI, 34, 299
- Chang, Q., Cuppen, H. M., Herbst, E., 2005, A&A, 434, 599
- Chang, Q., Cuppen, H. M., Herbst, E., 2007, A&A, 469, 973
- Charnley, S.B., 2001, ApJ, 562L, 99
- Cuppen, H. M., Herbst, E., 2007, APJ, 668, 294
- Cuppen, H. M., van Dishoeck, E. F., Herbst, E., Tielens, A. G. G. M., 2009, A&A, 508, 275
- Das, A., Acharyya, K., Chakrabarti, S., Chakrabarti, S. K., 2008, A & A, 486, 209
- Das, A., Acharyya, K., Chakrabarti, S., Chakrabarti, S. K., 2008, New Astronomy, 13, 457
- De Grauw, *et al.*, 1996, A&A, 315L, 345

- Farebrother, A.J., Meijer, A.J.H.M., Clary, D.C., Fisher, A.J., 2000, *Chem. Phys. Lett.*, 319, 303
- Fuchs, G. W. *et al.*, 2009, *A&A*, 505, 629
- Gillett, F. C., Forrest, W. J., 1973, *ApJ*, 179, 483
- Green, N. J. B *et al.*, 2001, *A&A*, 375, 1111
- Hasegawa, T., Herbst, E., Leung, C.M., 1992, *APJ*, 82, 167
- Hasegawa, T., Herbst, E., 1993, *MNRAS*, 261, 83
- Herbst, E., Klemperer, W., 1973, *APJ*, 185, 505
- Hollenbach, D., Salpeter, E. E., 1970, *J. Chem. Phys.*, 53, 79
- Hiraoka, K. *et al.*, 2002, *ApJ*, 577, 265
- Ioppolo, S., Cuppen, H. M., Romanzin, C., van Dishoeck, E. F., Linnartz, H., 2008, *ApJ*, 686, 1474
- Jørgensen, J. K., Schöier, F. L., van Dishoeck, E. F., 2002, *A&A*, 389, 908
- Keane, J. V., Boogert, A. C. A., Tielens, A. G. G. M., Ehrenfreund, P., Schutte, W. A., 2001, *A&A*, 375L, 43
- Lis, D. C. *et al.*, 2001, *ApJ*, 561, 823
- Pirronello, V., Biham, O., Liu, C., Shena, L., Vidali, G., 1997a, *ApJ*, 483L, 131
- Pirronello, V., Liu, C., Shena, L., Vidali, G., 1997b, *ApJ*, 475L, 69
- Pirronello, V., Liu, C., Riser, J. E., Vidali, G., 1999, *A&A*, 344, 681
- Prasad, S. S., Huntress, W. T., 1980a, *ApJS* 43, 1
- Roberts, H., Herbst, E., 2002, *A&A*, 395, 233
- Ruffle, D. P., Herbst, E., 2000, *MNRAS*, 319, 837
- Stantcheva, T., Shematovich, V. I., Herbst, E., 2002, *A&A*, 391, 1069
- Stantcheva, T., Herbst, E., 2004, *A&A*, 423, 241
- Tielens, A. G. G. M., Tokunaga, A.T., Geballe, T.R., Baas, F., 1991, *ApJ*, 381, 181
- Tielens, A. G. G. M., Allamandola, L.J., 1987, in *Interstellar Processes*, eds. D.J. Hollenbach, J. H. A. Thronson (Dordrecht), 397
- Tielens, A. G. G. M., Hagen, W., 1982, *A&A*, 114, 245
- Watanabe, N., Kouchi, A. 2002, *ApJ*, 571, L173
- Watson, W. D., Salpeter, E. E., 1972, *ApJ*, 174, 321
- Watson, W. D., Salpeter, E. E., 1972, *ApJ*, 175, 659
- Wilson, T. L., Rood, R. T., 1994, *ARA&A*, 32, 191
- Shen, C. J., Greenberg, J. M., Schutte, W. A. van Dishoeck, E. F., 2004, *A&A*, 415, 203

Garrod, R. T., Wakelam, V., Herbst, E., 2007 A&A, 467, 1103

Cazaux, S., Caselli, P., Cobut, V., Le Bourlot, J.i, 2008, A&A 483, 495

Katz, N., Furmann, I., Biham, O., Pironello, V., Vidali, G., 1999, ApJ, 522, 305

**Table 1.** Initial Gas-phase abundances used

| Species | high ( $cm^{-3}$ ) | intermediate( $cm^{-3}$ ) | low ( $cm^{-3}$ ) |
|---------|--------------------|---------------------------|-------------------|
| H       | 1.10               | 1.15                      | 1.15              |
| O       | 7.0                | 0.75                      | 0.09              |
| CO      | 7.5                | 0.75                      | 0.075             |

**Table 2.** Energy barriers in degree Kelvin

| Species            | Substrate |       |                |       |                |       |                  |       |       |                   |                   |                    |                 |
|--------------------|-----------|-------|----------------|-------|----------------|-------|------------------|-------|-------|-------------------|-------------------|--------------------|-----------------|
|                    | Silicate  | H     | H <sub>2</sub> | O     | O <sub>2</sub> | OH    | H <sub>2</sub> O | CO    | HCO   | H <sub>2</sub> CO | H <sub>3</sub> CO | CH <sub>3</sub> OH | CO <sub>2</sub> |
|                    | $E_D$     | $E_D$ | $E_D$          | $E_D$ | $E_D$          | $E_D$ | $E_D$            | $E_D$ | $E_D$ | $E_D$             | $E_D$             | $E_D$              | $E_D$           |
| H                  | 350       | 350   | 45             | 350   | 45             | 350   | 650              | 350   | 350   | 350               | 350               | 350                | 350             |
| H <sub>2</sub>     | 450       | 30    | 23             | 30    | 30             | 30    | 440              | 450   | 450   | 450               | 450               | 450                | 450             |
| O                  | 800       | 480   | 55             | 480   | 55             | 55    | 800              | 480   | 480   | 480               | 480               | 480                | 480             |
| O <sub>2</sub>     | 1210      | 69    | 69             | 69    | 69             | 1000  | 1210             | 1210  | 1210  | 1210              | 1210              | 1210               | 1210            |
| OH                 | 1260      | 1260  | 240            | 240   | 240            | 240   | 3500             | 1260  | 1260  | 1260              | 1260              | 1260               | 1260            |
| H <sub>2</sub> O   | 1860      | 390   | 390            | 390   | 390            | 390   | 5640             | 1860  | 1860  | 1860              | 1860              | 1860               | 1860            |
| CO                 | 1210      | 1210  | 1210           | 1210  | 1210           | 1210  | 1210             | 1210  | 1210  | 1210              | 1210              | 1210               | 1210            |
| HCO                | 1510      | 1510  | 1510           | 1510  | 1510           | 1510  | 1510             | 1510  | 1510  | 1510              | 1510              | 1510               | 1510            |
| H <sub>2</sub> CO  | 1760      | 1760  | 1760           | 1760  | 1760           | 1760  | 1760             | 1760  | 1760  | 1760              | 1760              | 1760               | 1760            |
| H <sub>3</sub> CO  | 2170      | 2170  | 2170           | 2170  | 2170           | 2170  | 2170             | 2170  | 2170  | 2170              | 2170              | 2170               | 2170            |
| CH <sub>3</sub> OH | 2060      | 2060  | 2060           | 2060  | 2060           | 2060  | 2060             | 2060  | 2060  | 2060              | 2060              | 2060               | 2060            |
| CO <sub>2</sub>    | 2500      | 2500  | 2500           | 2500  | 2500           | 2500  | 2500             | 2500  | 2500  | 2500              | 2500              | 2500               | 2500            |

For the all species  $E_b = 0.3 E_D$  is used except the atomic hydrogen where  $E_b = 0.2857 E_D$  is used. For the reference please see the text.

**Table 3.** Surface Reactions in the H, O, and CO model

| Number | Reactions  | $E_a$ (K) |
|--------|--|-----------|
| 1      | H+H $\rightarrow$ H <sub>2</sub>                     |           |
| 2      | H+O $\rightarrow$ OH                                 |           |
| 3      | H+OH $\rightarrow$ H <sub>2</sub> O                  |           |
| 4      | H+CO $\rightarrow$ HCO                               | 2000      |
| 5      | H+HCO $\rightarrow$ H <sub>2</sub> CO                |           |
| 6      | H+H <sub>2</sub> CO $\rightarrow$ H <sub>3</sub> CO  | 2000      |
| 7      | H+H <sub>3</sub> CO $\rightarrow$ CH <sub>3</sub> OH |           |
| 8      | O+O $\rightarrow$ O <sub>2</sub>                     |           |
| 9      | O+CO $\rightarrow$ CO <sub>2</sub>                   | 1000      |
| 10     | O+HCO $\rightarrow$ CO <sub>2</sub> +H               |           |

**Table 4.** Relative abundances (absolute abundance) of the ice species after two million years

| Initial gas phase<br>Oxygen | Species            | Initial gas phase<br>CO=7.5(-5) | Initial gas phase<br>CO=3.75(-5) | Initial gas phase<br>CO=1.5(-5) |
|-----------------------------|--------------------|---------------------------------|----------------------------------|---------------------------------|
| 7.0(-5)                     | H <sub>2</sub> O   | 100 [5.3(-5)]                   | 100 [6(-5)]                      | 100 [6.4(-5)]                   |
|                             | CO                 | 3 [1.6(-6)]                     | 1 [6.1(-7)]                      | 0.5 [2.9(-7)]                   |
|                             | H <sub>2</sub> CO  | 0.2 [8.8(-8)]                   | 0.05 [3(-8)]                     | 0.02 [1.1(-8)]                  |
|                             | CH <sub>3</sub> OH | 116 [6.1(-5)]                   | 52.3 [3.2(-5)]                   | 20 [1.3(-5)]                    |
|                             | CO <sub>2</sub>    | 22.7 [1.2(-5)]                  | 8.6 [5.2(-6)]                    | 2.8 [1.8(-6)]                   |
|                             | O <sub>2</sub>     | 5 [2.6(-6)]                     | 3.6 [2.2(-6)]                    | 3 [2(-6)]                       |
| 1.05(-4)                    | H <sub>2</sub> O   | 100 [7.5(-5)]                   | 100 [8.8(-5)]                    | 100 [9.4(-5)]                   |
|                             | CO                 | 0.8 [5.8(-7)]                   | 0.4 [3.7(-7)]                    | 0.3 [2.4(-7)]                   |
|                             | H <sub>2</sub> CO  | 0.05 [4(-8)]                    | 0.01 [1.2(-8)]                   | 0.01 [7(-9)]                    |
|                             | CH <sub>3</sub> OH | 70.3 [5.3(-5)]                  | 33.4 [2.9(-5)]                   | 13 [1.2(-5)]                    |
|                             | CO <sub>2</sub>    | 20.7 [1.5(-5)]                  | 7.8 [6.8(-6)]                    | 2.5 [2.4(-6)]                   |
|                             | O <sub>2</sub>     | 7 [5.3(-6)]                     | 5.4 [4.7(-6)]                    | 4.6 [4.4(-6)]                   |
| 3.5(-4)                     | H <sub>2</sub> O   | 100 [2.1(-4)]                   | 100 [2.3(-4)]                    | 100 [2.1(-4)]                   |
|                             | CO                 | 0.1 [2.1(-7)]                   | 0.02 [4.5(-8)]                   | 0.02 [3.5(-8)]                  |
|                             | H <sub>2</sub> CO  | 0.01 [1.9(-8)]                  | 0.0 [4.8(-9)]                    | 0.0 [1.6(-9)]                   |
|                             | CH <sub>3</sub> OH | 19.4 [4.1(-5)]                  | 9.5 [2.2(-5)]                    | 3.3 [6.8(-6)]                   |
|                             | CO <sub>2</sub>    | 14.3 [3(-5)]                    | 6.2 [1.4(-5)]                    | 2.5 [5.2(-6)]                   |
|                             | O <sub>2</sub>     | 24.2 [5.1(-5)]                  | 21.7 [5(-5)]                     | 23.7 [4.9(-5)]                  |
| 7.0(-4)                     | H <sub>2</sub> O   | 100 [2.4(-4)]                   | 100 [3.4(-4)]                    | 100 [3.6(-4)]                   |
|                             | CO                 | 0.03 [8.4(-8)]                  | 0.02 [6.5(-8)]                   | 0.00 [3.7(-8)]                  |
|                             | H <sub>2</sub> CO  | 0.00 [1.2(-8)]                  | 0.00 [4.8(-9)]                   | 0.00 [1.1(-9)]                  |
|                             | CH <sub>3</sub> OH | 8.5 [2.2(-5)]                   | 4.9 [1.7(-5)]                    | 2 [7.1(-6)]                     |
|                             | CO <sub>2</sub>    | 15 [3.8(-5)]                    | 5.7 [2(-5)]                      | 2.1 [7.6(-6)]                   |
|                             | O <sub>2</sub>     | 63 [1.6(-4)]                    | 48.6 [1.7(-4)]                   | 46.8 [1.7(-4)]                  |

**Table 5.** Relative abundances of the ice species by assuming different activation barrier energy for H+CO and H+H<sub>2</sub>CO reactions in the intermediate initial abundance case

| Species            | 2000 | 3000 | 4000 | 5000 |
|--------------------|------|------|------|------|
| H <sub>2</sub> O   | 100  | 100  | 100  | 100  |
| CO                 | 3    | 2.2  | 15.6 | 85.3 |
| H <sub>2</sub> CO  | 0.2  | 0.06 | 0.5  | 0.2  |
| CH <sub>3</sub> OH | 116  | 111  | 95   | 19.4 |
| CO <sub>2</sub>    | 22.7 | 19   | 7    | 1.5  |
| O <sub>2</sub>     | 5    | 5.4  | 5    | 5.3  |

**Table 6.** Relative abundances of the ice species in different regions of the interstellar cloud

| Species            | Low  | Intermediate | High |
|--------------------|------|--------------|------|
| H <sub>2</sub> O   | 100  | 100          | 100  |
| CO                 | 0.7  | 3            | 160  |
| H <sub>2</sub> CO  | 0.02 | 0.2          | 13   |
| CH <sub>3</sub> OH | 68   | 116          | 146  |
| CO <sub>2</sub>    | 2.5  | 23           | 143  |
| O <sub>2</sub>     | 0.5  | 5            | 96   |

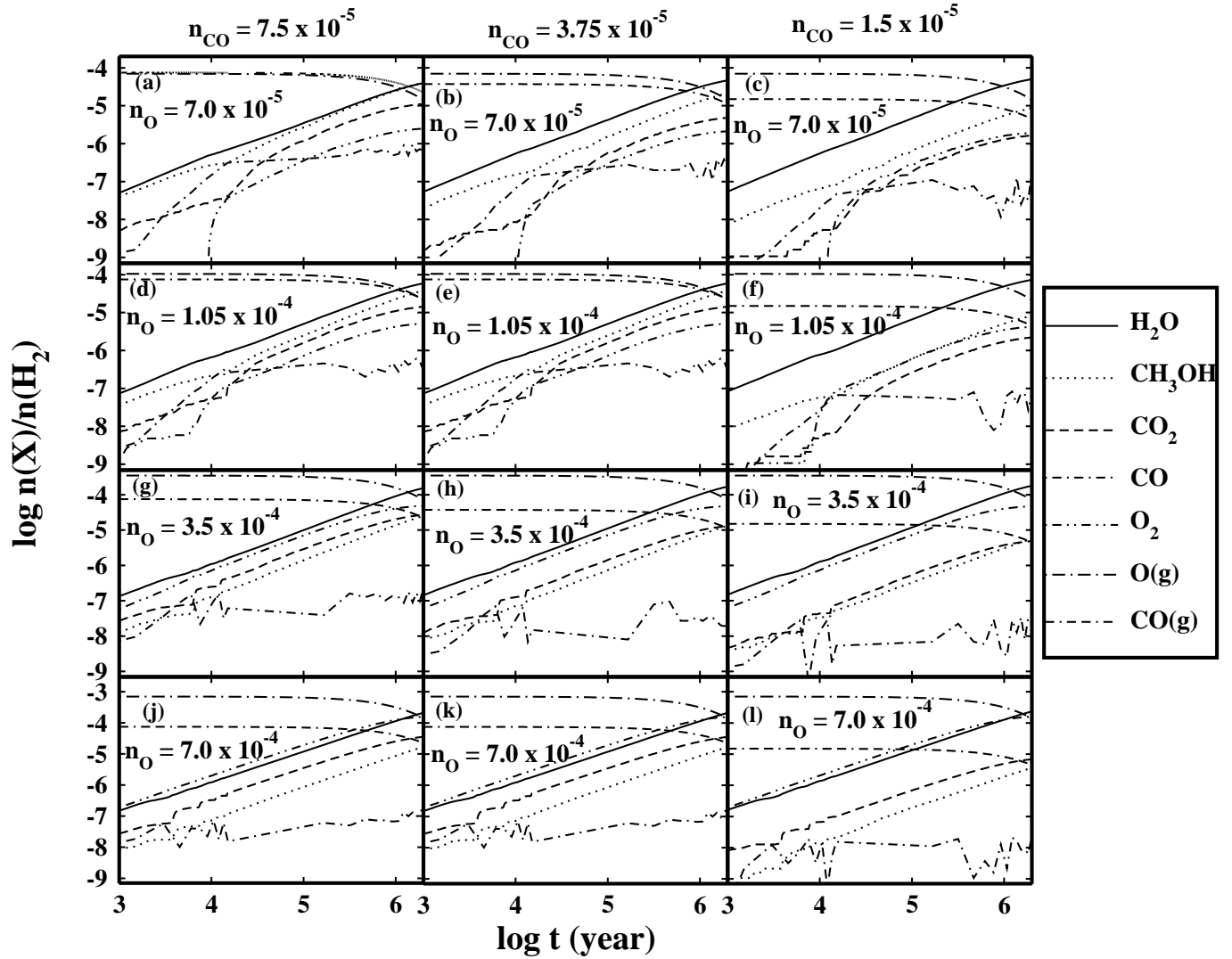
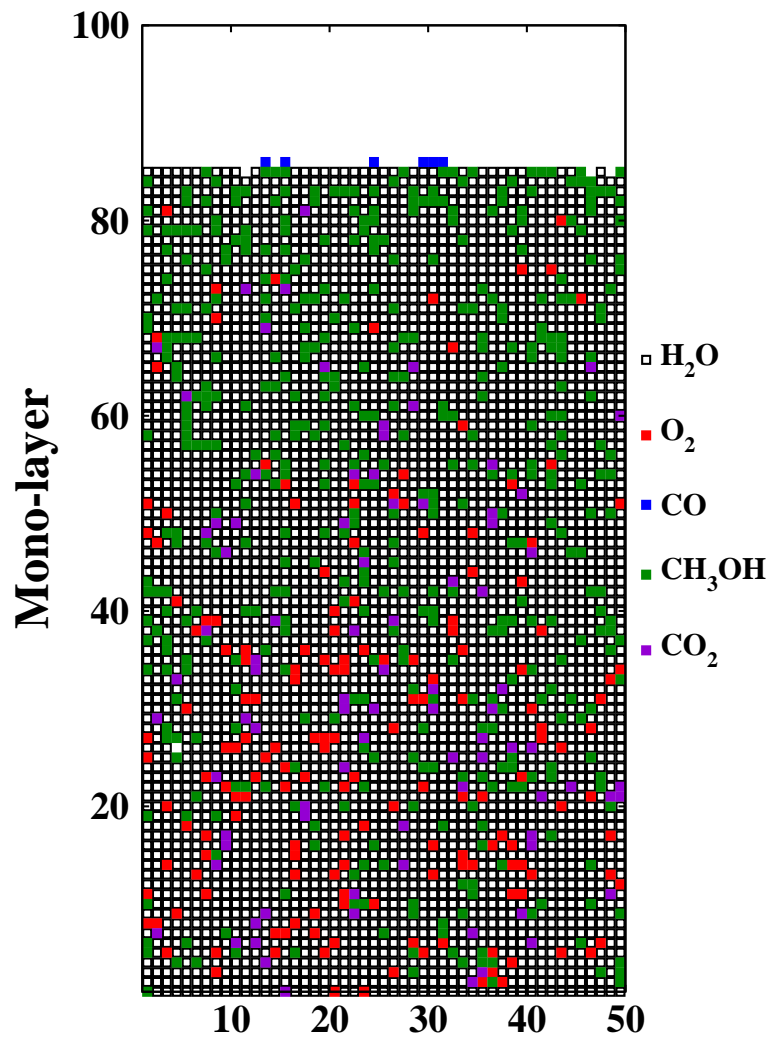


Figure 1. Time variation of major grain surface species for different initial abundance of carbon monoxide and oxygen. Chosen CO abundances are  $7.5 \times 10^{-5}$  (1<sup>st</sup> column),  $3.75 \times 10^{-5}$  (2<sup>nd</sup> column) and  $1.5 \times 10^{-5}$  (3<sup>rd</sup> column).



**Figure 2.** A cross-sectional view of the grain mantle after one million years for initial O and CO abundance of  $1.05 \times 10^{-4}$  and  $1.5 \times 10^{-5}$  respectively.

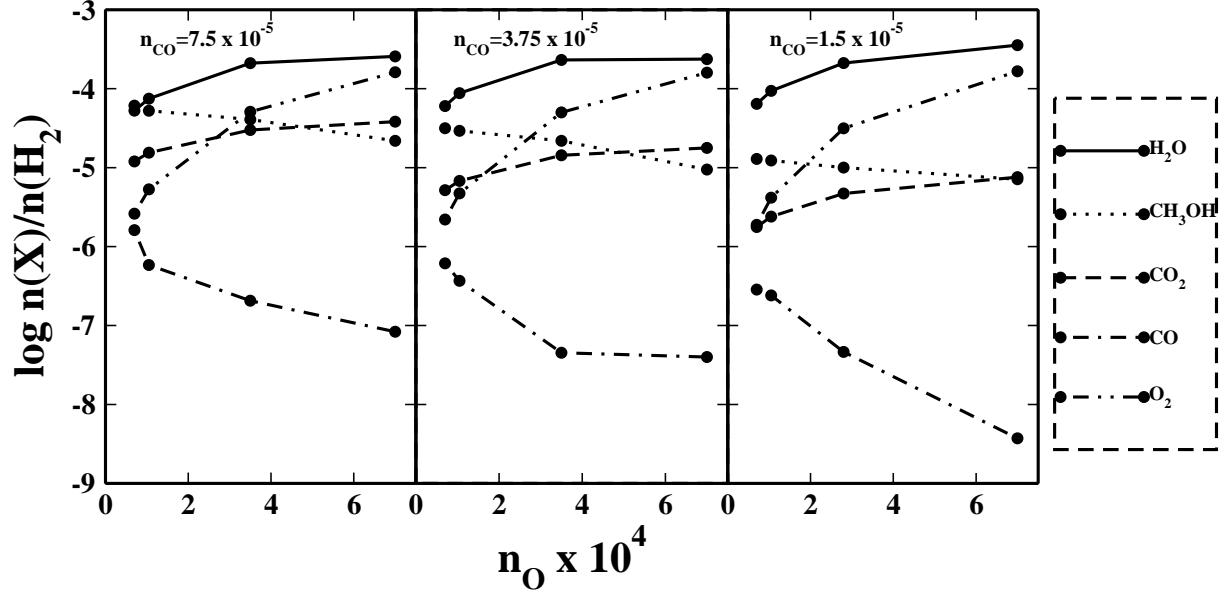


Figure 3. Variation of the final mantle abundance of the selected species as a function of initial abundance of gas phase O.

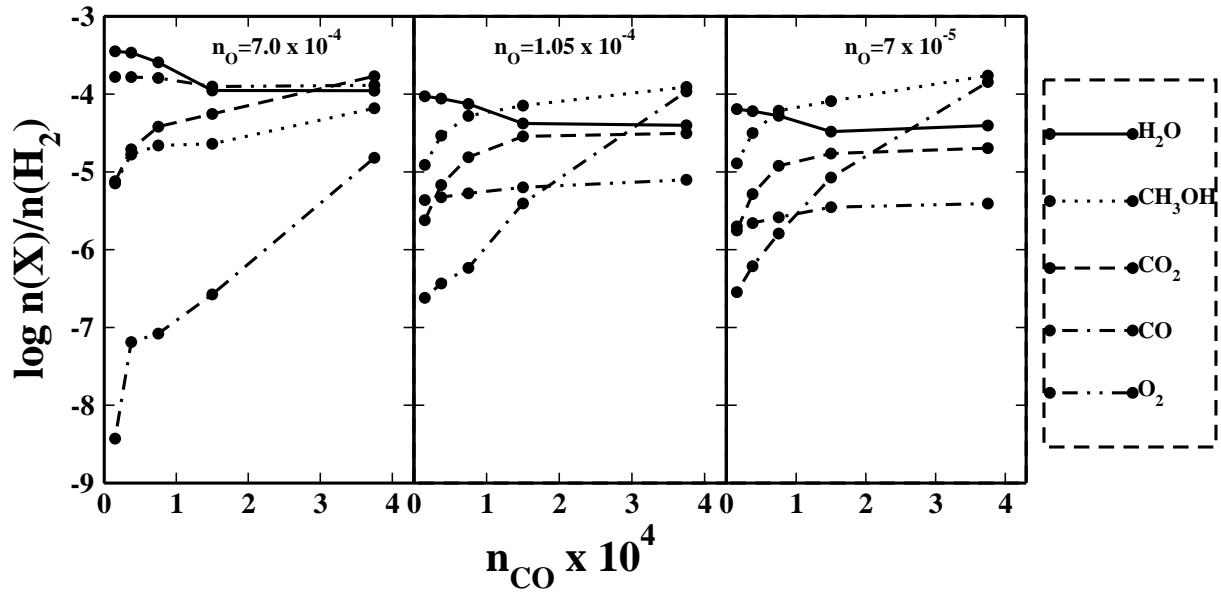
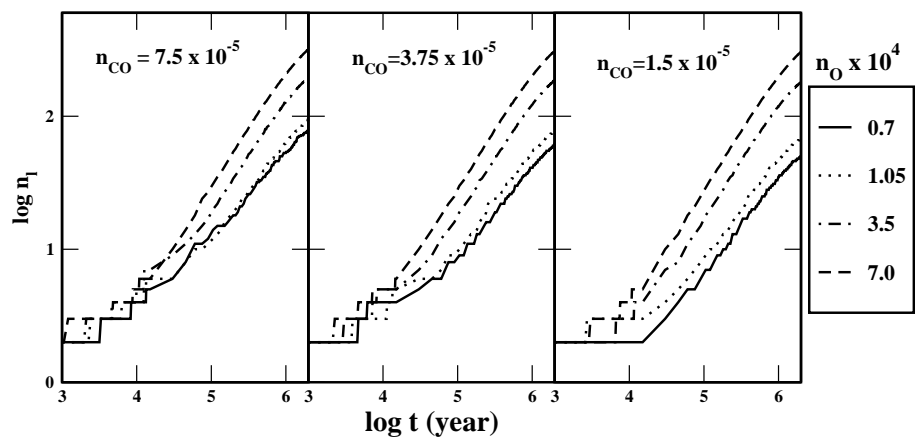
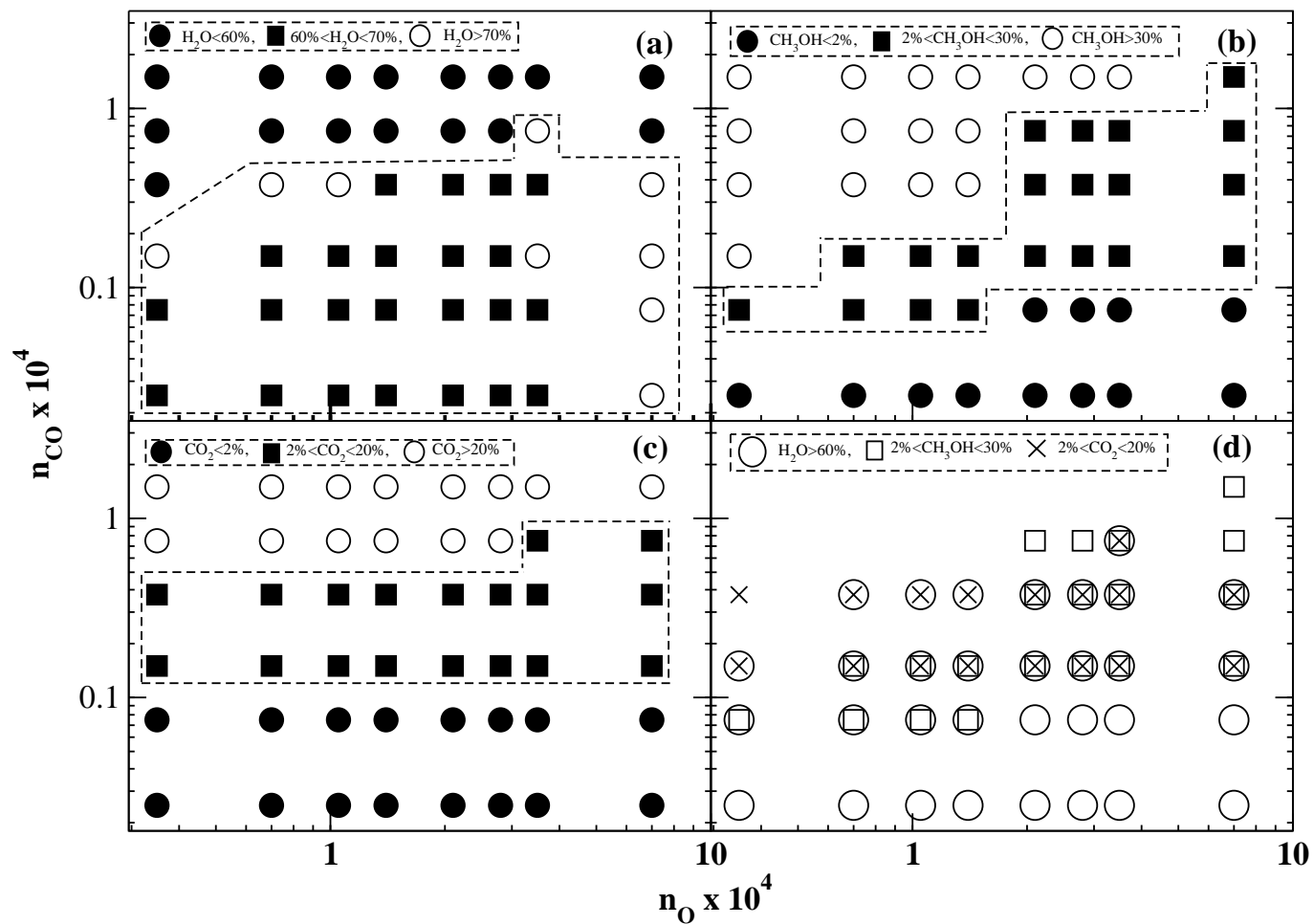


Figure 4. Variation of the final mantle abundance of selected species as a function of initial abundance of gas phase CO.



**Figure 5.** Time Variation of grain mantle thickness (in mono-layers) as function of initial O and CO abundance.



**Figure 6.** The parameter space in which formations of water, methanol and  $\text{CO}_2$  are studied. The regions in which these molecules are produced **within the observed limits** (favourable zones) is marked on the parameter space. (d) Favourable zone is the common zone when (a-c) are superimposed.

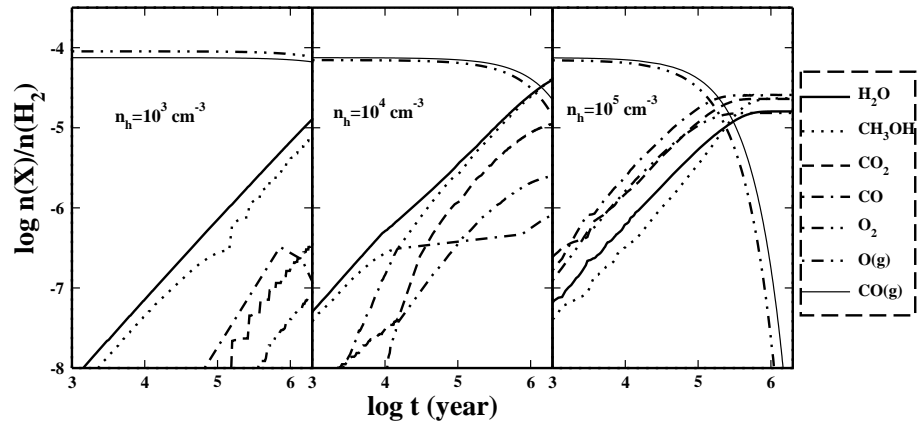


**Figure 7.** Time evolution of selected species for various cloud densities.

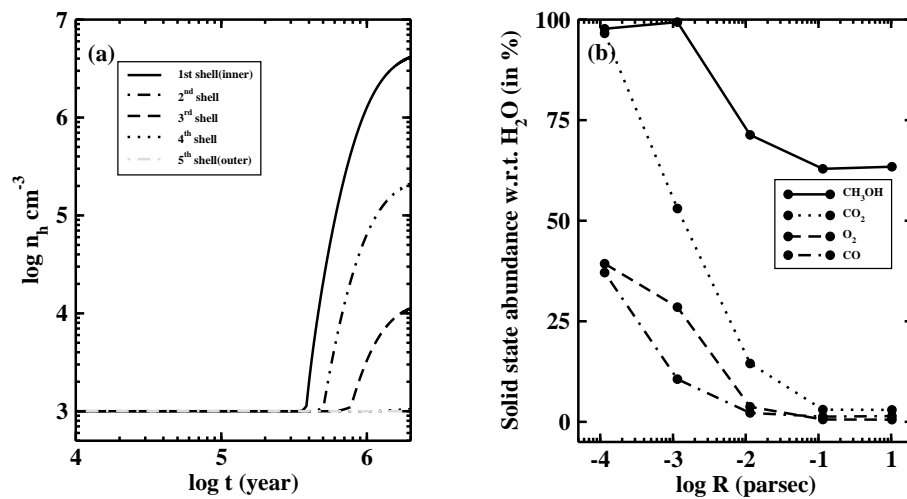


**Figure 8.** Time evolution of (a) gas number density and (b) final abundances of some selected species in different region of a collapsing cloud.

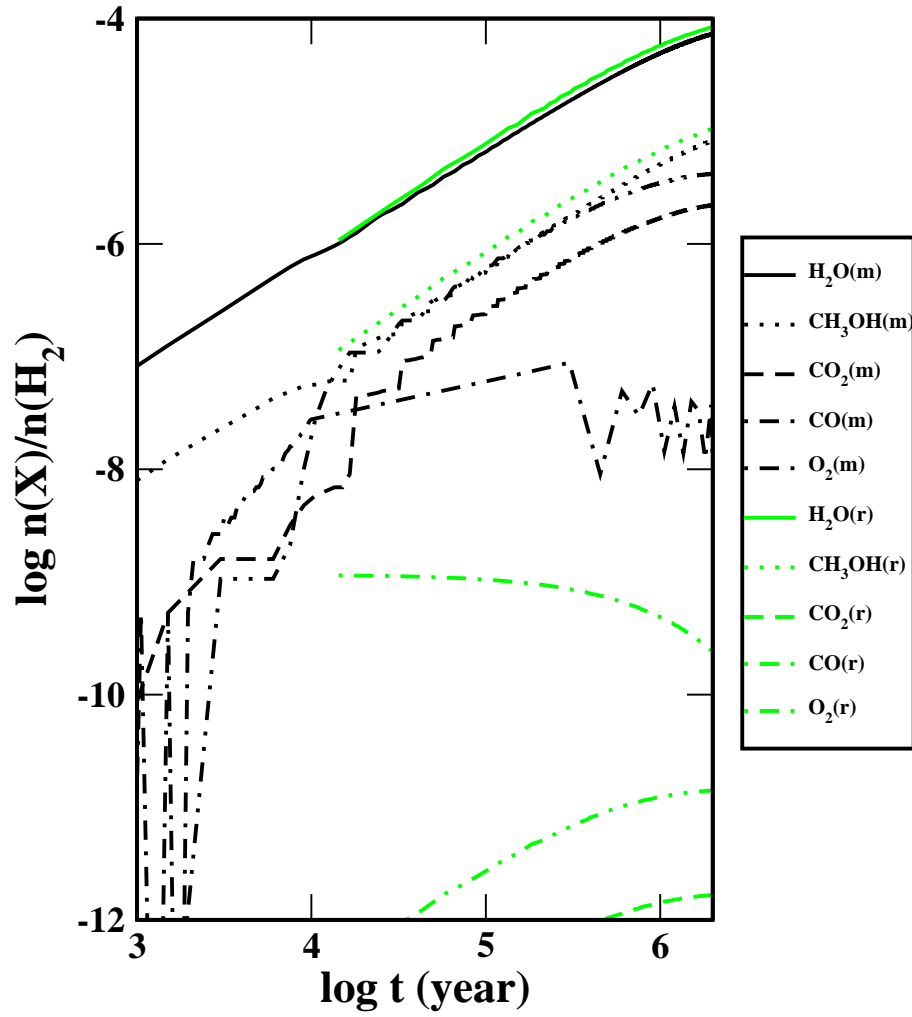


Figure 9. Comparison of results from Monte Carlo simulation (m) and rate equation (r) methods.